Biosensors and Bioelectronics 168 (2020) 112527

Contents lists available at ScienceDirect

Biosensors and Bioelectronics

journal homepage: http://www.elsevier.com/locate/bios

Electrochemical biosensor for rapid detection of bacteria based on facile synthesis of silver wire across electrodes

Ye Feng [a], Dan Zhou [a], Lujia Gao [b], Fengjiao He [a,*]

[a] State Key Laboratory of Chemo/Biosensing and Chemometrics, College of Chemistry and Chemical Engineering, Hunan University, Changsha, 410082, China
[b] Chemistry Department, Reed College, Portland, 97202, USA

ARTICLE INFO

Keywords:
16S ribosomal-RNA
Bacteria
Staph. aureus
MSPQC
HCR

ABSTRACT

The early detection of bacteria is of critical importance in addressing serious public health problems. Here, an electrochemical biosensor for rapid detection of bacteria based on facile synthesis of silver wire across electrodes was constructed. High-variable region of 16S rRNA of bacteria was used as biomarker. Polymerase-free synthesis of silver wire was introduced into electrochemical signal transduction to improve the sensitivity of electrochemical detection. The construction biosensor of proposed method is as follows: Metastable hairpin probe H_1 was modified on electrode surface, biomarker can open the stem-loop structure of H_1 and activates HCR. The alternate opening of the stem-loop structure of H_1 and H_2-AuNPs finally results in the formation of long double-stranded DNA-RNA (HCR products) -AuNPs. The formed AuNPs modified HCR products was blown in one direction using N_2 to across the electrode gap. Using this HCR products as template, the silver wire was formed between the electrodes by silver deposition, and resulted in sharp change in electrical parameters of electrode. As the proof-of-concept work, multichannel series piezoelectric quartz crystal (MSPQC) was utilized as detector. The detection of *Staphylococcus aureus* in the concentration range from 50 to 10^7 CFU/mL within 100 min was achieved. The detection limit was 50 CFU/mL. *Escherichia coli*, *Salmonella enteritidis*, *Listeria innocua*, *Pseudomonas aeruginosa* and *Streptococcus pneumoniae* did not interfere the detection results. This newly proposed electrochemical biosensor is simple, rapid and exhibit high signal-to-noise ratio, it has great potential for being applied in food safety monitoring and clinical diagnosis.

1. Introduction

Rapid qualitative and quantitative detection of bacteria has many potential applications in clinical diagnosis, environmental monitoring and food safety(Furst and Francis, 2019). Traditional culture method, which used as the gold standard approach for bacteria detection, is limited by the tedious process and false-positive signal which caused by uncultivated bacteria(Davenport et al., 2017). Above-mentioned limitation of culture method have led to the development of molecular biological techniques which based on a variety of biomarkers (e.g. antibodies (Kim et al., 2018; Stobiecka et al., 2019), nucleic acids (Stobiecka and Chalupa, 2016; Tavallaie et al., 2018), enzymes (Adkins et al., 2017) etc.,) and signal detectors (including optical (Aman et al., 2020), fluorescent (He et al., 2020; Martynenko et al., 2019; Ratajczak et al., 2019, 2018; Stobiecka et al., 2012), chromatographic (Ratajczak and Stobiecka, 2020; Stobiecka and Chałupa, 2015), electrochemical (Ranjbar et al., 2019) and piezoelectric (Feng et al., 2019; Milioni et al., 2020)-triggered molecules). Owing to their characteristic of free-culturing, it is expected to improve the positive detection rate and shorten the detection time. However, most methods are still limited by long processing time (over 18 h from sampling to results), expensive instruments and skilled technicians(Imai et al., 2019; Slomovic et al., 2015). Accordingly, the rapid, simple, reliable method for bacteria detection in the early stage of bacterial infections remains an urgent need(Peng and Chen, 2019).

Bacterial 16S rRNA is of high universality and abundance in bacteria and provides rich genetic information(Wang et al., 2019). Currently, 16S rRNA has been recognized as a specific target and extensively used for the identification of bacteria. Polymerase chain reaction (PCR) combined with 16S rRNA gene sequencing is commonly used bacteria detection technique, it is capable of classifying unknown strains(Bauza et al., 2019; Deshmukh et al., 2019). But the processing time, expensive instrument and operator requirements have restricted the application of this method in point-of-care settings(Tavallaie et al., 2018).

* Corresponding author.
E-mail address: fengjiaohe@hnu.edu.cn (F. He).

https://doi.org/10.1016/j.bios.2020.112527
Received 14 July 2020; Received in revised form 13 August 2020; Accepted 19 August 2020
Available online 22 August 2020

Hybridization chain reaction (HCR) is an isothermal enzyme-free amplification strategy which can assemble hairpins into long double-stranded nucleic acids(Figg et al., 2020). In the presence of the initiator, it binds to one hairpin and initiates the alternate opening of the stem-loop structure of two hairpins, finally resulting in the formation of long linear double-stranded DNA nanostructure with a large amount of repetitive sequence units(Wu et al., 2019). HCR is usually used as signal amplification technique for nucleic acids analysis by combining signal molecules with repeating units of HCR products (Augspurger et al., 2018; Wang et al., 2020).

Electrochemical techniques are the suitable point-of-care techniques due to their fast response, easy readout, portability, and low cost(Reta et al., 2018; Zhang et al., 2019). In a typical electrochemical method, the signal conversion is based on the change of the concentration of signal molecules on the electrode surface, thus they are suffered from background noise problem (which caused by the aggregation between signal molecules) and limited detection reproducibility in complex media such as food or whole blood(Amiri et al., 2018). Overall, the lack of efficient signal conversion strategy hinders the application of conventional electrochemical sensors in the field of point-of-care(Bai et al., 2004; Furst and Francis, 2019). Thus, a highly effective signal conversion strategy that offers low background noise and high reproducibility needs to be developed to enable the application of electrochemical technology to molecular diagnostics platforms.

In this paper, an electrochemical biosensor for rapid detection of bacteria based on facile synthesis of silver wire across electrodes was proposed. Fragment of bacterial 16S rRNA hyper-variable region was used as biomarker and HCR combined with silver deposition technique was used to form silver wire crossing electrode. We introduced polymerase-free synthesis of silver wire into electrochemical signal conversion to improve the sensitivity of electrochemical detection. Using the reported 16S rRNA fragment of *Staphylococcus aureus* (*Staph. aureus*) as the target (Hwang et al., 2012), the proposed biosensor achieved the detection of *Staph. aureus* as low as 50 CFU/mL in 100 min. This potent detection strategy is simple, portable and rapid, it expected to become a universal multiplexing detection platform of bacteria, and might find widely use in the fields of public safety and early diagnosis.

2. Experimental section

2.1. Materials and equipment

Staph. aureus was purchased from the National Institute for the Control of Pharmaceutical and Products. TNT (100 mmol/L Tris-HCl; 1.5 mol/L NaCl; 0.5% Tween 20), Sodium lauryl sulfate (SDS), SPSC buffers (50 nM Na_2HPO_4 pH = 6.5, 1 M NaCl), agarose gels are purchased from Sangon Biotech. Co., Ltd. (Shanghai, China). Tris-(2-carboxyethyl)-phosphine hydrochloride (TCEP) are purchased from BBI. LI silver enhancement kit is purchased from Nanoprobes (USA). All reagents were analytical reagent grade.

The interdigital electrode with 20 μm electrode gap was bought from Dalian Institute of Chemical Physics, the detailed parameters are shown in supplementary information section 1.

MSPQC system is self-constructed, the equipment construction and sensing mechanism are listed in supplementary information section 2, the detailed parameter setting is shown in supplementary information section 3.

All used sequences are listed in Table 1. The sequences are synthesized by Shanghai Sangon Biological Engineering Technology and Services, Co., Ltd. (Shanghai, China) and used without further purification.

For characteristics, all used apparatus include high-resolution transmission electron microscope JEM-3010 (Japan Electronics Corporation, Japan), scanning electron microscope Hitachi S-4800 (Japan Hitachi Limited, Japan).

Table 1
Sequences of probes and biomarker.

Function	Sequence (5′-3′)
Biomarker	CCUGGAAUUCUACCCCCCUCUACA
H_1[a]	HS-tgtagaGGGGGGTAGAATTCCAGG*CAAAGT*CCTGGAATTCTACCCCCC
H_2[a]	HS-CCTGGAATTCTACCCCCC*TCTACA*GGGGGGTAGAATTCCAGGactttg
For specificity test	
$Random_r$	UAAACGGUUUAAACGGGAAAUAGC
$Mismatch_1$	CCUGGAAUUCUUCCCCCCUCUACA
$Mismatch_2$	CCUGGAAUUCUUUCCCCCUCUACA
$Mismatch_3$	CCUGGAAUUCUUUUCCCCUCUACA

[a] The sticky ends are in lower case. The loop parts are in italics. $Biomarker_r$ represents random sequences, $biomarker_1$, $biomarker_2$, $biomarker_3$ represents the sequence with 1 nt, 2 nt and 3 nt mismatch sites compared with Biomarker, separately.

2.2. Preparation of electrode and reagents

Modification of H_2 on AuNPs: 80 nm AuNPs were prepared according to Jenkin's method(Jenkins et al., 2017). H_2 modification on AuNPs was processed by following procedures: 3 μM reduced H_2 was added into AuNPs solution and incubated for 12 h at 4 °C. 0.05 M NaCl solution was added and aged for 12 h. Excess NaCl was removed by centrifuge at 12, 000 rpm for 25 min. H_2-modified AuNPs were washed 3 times by 0.01 M phosphate buffer solution (pH 7.4) and then resuspended in 0.5 mL SPSC buffer (pH 6.5).

HCR buffer: Prepared by 1 μM H_1 and 1 μM hairpin 2 modified AuNPs (H_2-AuNPs) in SPSC buffer.

Modification of interdigital electrode: The interdigital electrode was treated with warm Piranha solution (30% hydrogen peroxide and 70% concentrated sulfuric acid) for 10 s, ultrasonically cleaned with ethanol and acetone for 5 min orderly, then rinsed with double-distilled water and dried. H_1 was self-assembled on gold electrode by incubated in SPSC buffer (pH 6.5) containing 1 μM H_1 overnight at 4 °C. The electrode was washed by double-distilled water, and immersed in 1 μM mercaptoethanol (MCH) overnight at 4 °C and then was washed by double-distilled water and dried by N_2.

2.3. Detection of bacteria

Treatment of sample solution: the concentration of *Staph. aureus* was measured by plate counting, $(1.4 \pm 0.2) \times 10^8$ CFU/mL, and it was diluted to 1-10^7 cfu/mL with sterile saline. Taking 1 mL sample solution, centrifuged in 8000 rpm for 1 min, dissolving precipitate in 80 μg/mL lysozyme and standing for 10 min. Now the sample is ready for use.

Detection of bacteria: Adding 1 mL pretreated sample solution to the detection cell with aseptic operation, incubating for 30 s at room temperature, followed by adding 1 mL HCR buffer to the detection cell which contain interdigital electrode and recording the initial frequency (F_0). Taking out the solution from the detection cell with a syringe, and washing cell with 0.1 × TNT and 0.1% SDS. Connect the needle of syringe with nitrogen cylinder, place the needle parallel to the plane of the electrode, and perpendicular to the electrodes. Drying electrode with N_2 airflow. Taking 1 mL reduction solution from LI silver enhancement kit to detection cell and standing for 5 min; adding the enhancement solution to detection cell and stand for 5 min; recording oscillator frequency (F). The frequency shift (ΔF, $\Delta F = F–F_0$) were calculated. The concentration of bacteria can be calculated according to ΔF value.

3. Results and discussion

3.1. The constructive strategy of biosensor

Since the variable region of 16S rRNA reflects the difference among

species, the highly specific fragment of *Staph. aureus* 16S rRNA was selected as the biomarker(Hwang et al., 2012). The principle of constructed method was depicted in Scheme 1. The interdigital electrode was modified with hairpin 1 (H_1) by Au–S bond. H_1 and hairpin 2 (H_2) are two metastable hairpin probes required for HCR amplification. They have a stem of 18 bp, a loop of 6 nt, and a sticky end of 6 nt. The sequence of the sticky end and stem of H_1 is complementary to the biomarker. The sequence of sticky end and stem of H_2 is complementary to the loop and stem of H_1. Dropping sample solution onto the interdigital electrode and incubated for a while. Then adding HCR buffer solution which contain H_1 and AuNPs-H_2 onto the electrode surface. In the absence of biomarker, H_1 and AuNPs-H_2 coexist stably in solution. H_1 which modified on electrode remains stem-loop structure. In the presence of biomarker, the stem-loop structure of H_1 modified on electrode is opened and HCR process in HCR buffer is activated. The opened H_1 immediately hybridizes with H_2-AuNPs and opens the hairpin structure of H_2. The alternate opening of the stem-loop structure of H_1 and H_2 finally results in the formation of a long linear double-stranded DNA-RNA (HCR products) modified AuNPs on electrode. Washing the electrode surface with anionic surfactants SDS, then blowing the electrode surface with N_2, HCR products modified AuNPs are extended and crossed the interdigital electrode gap. Adding silver solution to electrode, the conductive silver wires are formed along HCR products by using AuNPs as nucleation sites. Eventually, the presence of biomarker changed the link between interdigital electrodes from the original non-conductive link to conductive silver link. This change in electrical parameter between electrodes could be simply measured by corresponding equipment. As a proof-of-principle work, here MSPQC equipment was used as the detector.

3.2. Verification of biosensor for bacteria detection

The formation of HCR products and silver wire between adjacent finger electrodes are two key procedures, which were directly related to the feasibility of proposed biosensor. Agarose gel electrophoresis, transmission electron microscopy (TEM), scanning electron microscope (SEM) were used to characterize the formation of HCR products and silver wire between finger electrodes.

Fig. 1a showed the HCR results of agarose gel electrophoresis. Lanes 1–3 represented HCR results of solution containing H_1, H_1+H_2, H_1+H_2+biomarker, respectively. Obviously, HCR products which exhibited stepped continuous bands only formed in the solution containing H_1+H_2+biomarker.

Fig. 1b and c were TEM images of H_2-AuNPs with different magnification, respectively. The translucent and uniform DNA layer on AuNPs shown in Fig. 1c suggested the successful modification of H_2 on AuNPs. Fig. 1d was TEM image of HCR products, the regular linear arrangement of AuNPs indicated that H2-AuNPs were hybridized with H1 to form HCR products. Otherwise, AuNPs would be arranged randomly as shown in Fig. 1b.

Fig. 1e and f were SEM images of electrodes after the process of HCR and silver deposition in presence and absence of biomarker, respectively. It can be seen that in the presence of biomarker, the silver wire which crossing the electrode gap was formed (Fig. 1e). In the absence of biomarker, the silver wire did not form between electrodes (Fig. 1f).

In summary, HCR products and silver wire which crossing adjacent finger electrodes were formed when target exists, confirming the success of the designed biosensor.

3.3. Evaluation of the effect of biosensor

3.3.1. The effect of HCR time on detection of bacteria

The time of HCR would affect the length of product. In designed detection method, the length of HCR product should be long enough to span the adjacent finger electrode. Fig. 2 showed the SEM images of the interdigital electrode after silver deposition when HCR time is 10 min, 30 min, 45 min and 75 min. The results indicate that when HCR time is more than 75 min, the length of HCR product can span 20 μm electrode gap. The effect of HCR time on frequency change was shown in Fig. 2e. When HCR time was increased from 10 min to 45 min, there was little change in frequency. As HCR time increased to 60 min, the frequency change increased sharply, and reached a plateau after 75 min. Thus, 75 min was selected as the optimal HCR time.

3.3.2. The effect of AuNPs size on bacteria detection

In order to optimize the performance of proposed method, 14 nm, 50 nm, 80 nm, 100 nm were used to investigate the effect of AuNPs particle size on detection of bacteria. The UV spectrum of AuNPs was shown in Fig. 3a. It can be seen in Fig. 3a that increased particle size caused the maximum wavelength red shift. The experimental results of proposed method were shown in Fig. 3b. When AuNPs size was less than 80 nm, the frequency change increased gradually with the increase of AuNPs size. After AuNPs diameter was larger than 80 nm, the frequency change decreased with the increase of AuNPs size. This might be due to the fact that the larger the size of gold nanoparticles as the core of silver deposition, the more likely the silver growth to form continuous silver wires.

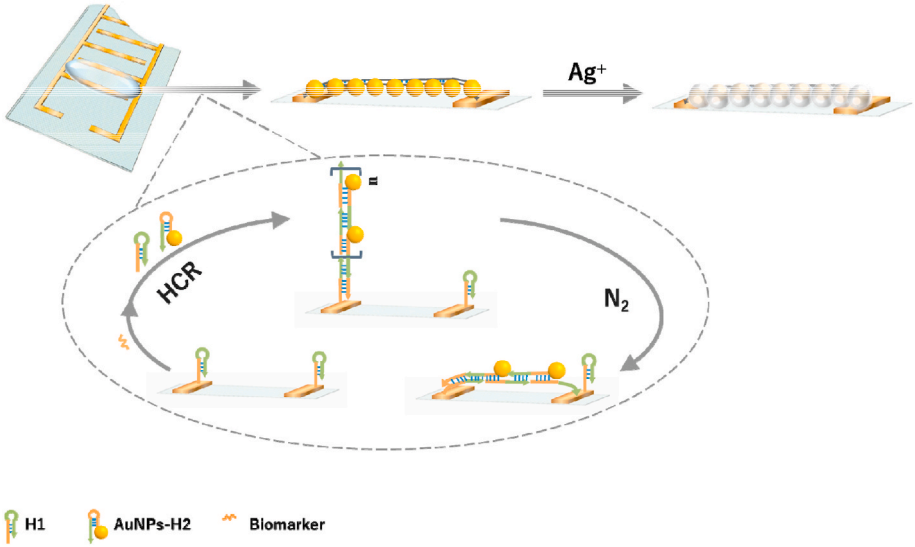

Scheme 1. The construction strategy of method for bacteria detection.

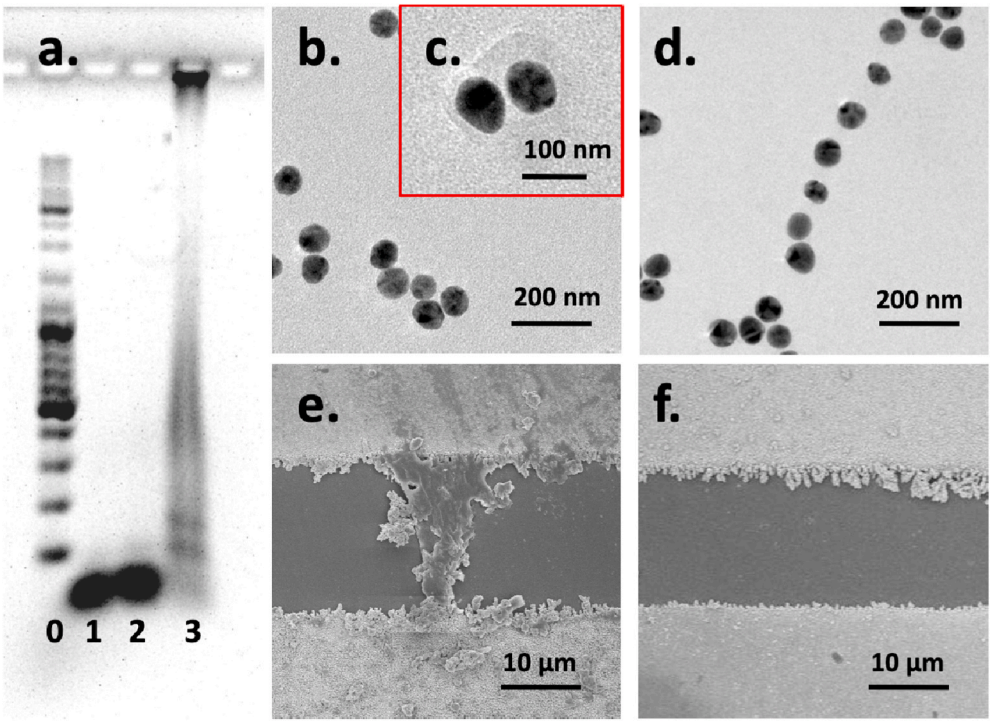

Fig. 1. Verification of the proposed biosensor for bacteria detection. (a) The gel-electrophoresis figure of HCR products. Lanes 0–3 represent DNA ladder marker (100–10000 bp), H_1, H_1+H_2, H_1+H_2+biomarker. (b) TEM image of AuNPs-DNA conjugates. (c) TEM image of AuNPs-DNA conjugates in high magnification. (d) TEM image of AuNPs-bounded HCR products. (e) SEM image of the positive sample after silver deposition. (f) SEM image of the control electrode after silver deposition.

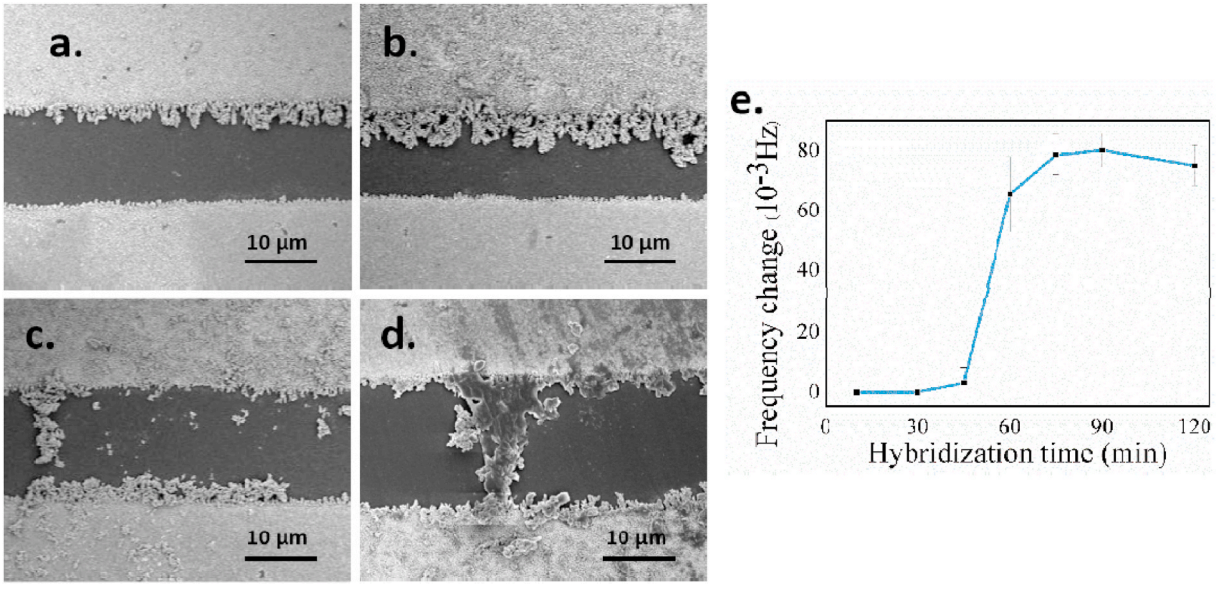

Fig. 2. SEM images of interdigital electrode as the hybridization time is (a.) 10 min, (b.) 30 min, (c.) 45 min, (d) 75 min. (e) The frequency change over HCR time. 75 min was selected as the optimal HCR time.

However, because H2-AuNPs were used to form DNA double helix structure, if the size of AuNPs is too large, the formation of long HCR products will be affected due to the large torsion force and steric hindrance effect. Here 80 nm was selected as the optimum diameter of AuNPs.

The TEM image of AuNPs with the diameters of 14 nm, 50 nm, 80 nm, 100 nm were shown in Figure S-3.

3.3.3. *Evaluation of the specificity of biomarker*

The specificity of constructed method for biomarker was evaluated by detecting random sequences, sequence with 1 nt, 2 nt, and 3 nt mismatch bases compared with specific biomarker, concentration all at 1×10^5 CFU/mL. The detection results were shown in Fig. 4. The degree of interference (DI) of five interfering bacteria to *Staph. Aureus* can be evaluated by formula (1):

$$DI = \Delta F_I / \Delta F_T \times 100\% \quad (1)$$

Where ΔF_I and ΔF_T were represented the frequency change of six samples and target sequence (Biomarker). The DI values for random

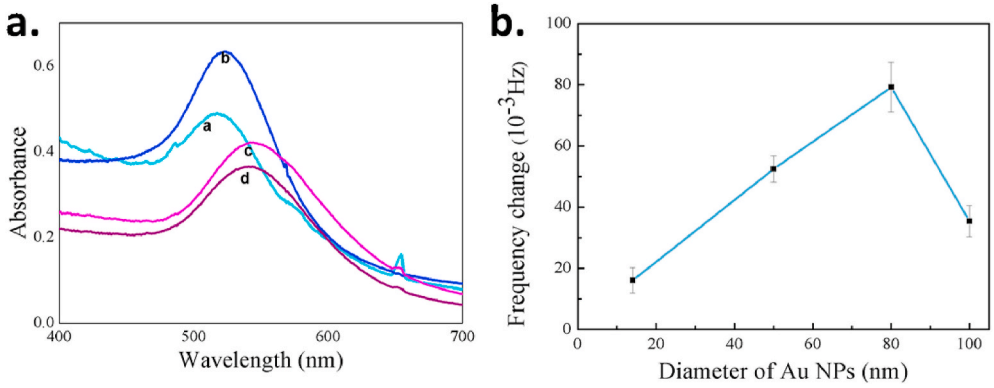

Fig. 3. a. UV spectra images of (a) 14 nm, (b) 50 nm, (c) 80 nm, (d) 100 nm AuNPs. b. The effect of AuNPs size on detection of target bacteria.80 nm was selected as the optimum diameter of AuNPs.

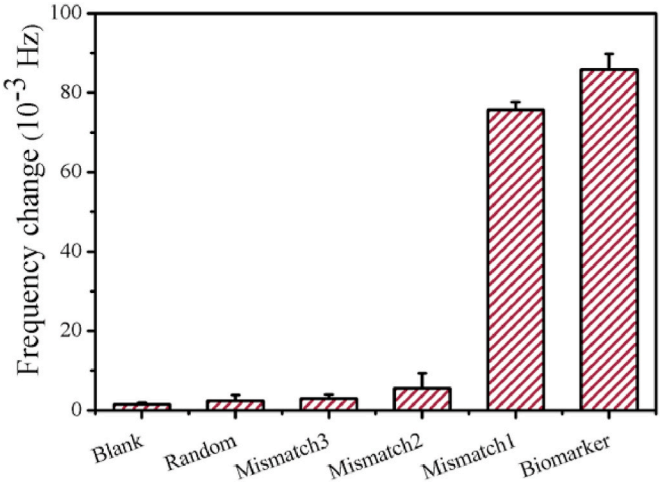

Fig. 4. The effect of interfering sequences to specific biomarker.

sequences (Random), sequence with 1 nt ($Mismatch_1$), 2 nt ($Mismatch_2$), and 3 nt ($Mismatch_3$) mismatch bases compared with specific biomarker were 1.04%, 3.56%, 4.87%, and 87.89% respectively, indicating that besides the single-base mismatches sequences, the interference of other non-specific nucleic acids to detection of biomarker could be negligible.

The above results revealed that proposed method could detect double-base mismatches. This might be due to the fact that although the design of the sensor avoids the signal interference caused by nonspecific adsorption, but nucleic acid hybridization itself allows a certain degree of base mismatch, thus, the proposed sensor based on nucleic acid hybridization cannot realize the detection of single base mismatch.

3.4. Detection of bacteria

3.4.1. The relationship between frequency change and the concentration of bacteria

In order to evaluate the quantification capability of the as-developed method for bacterial detection, simulated sample with *Staph. Aureus* at a concentration ranging from (1.4 ± 0.2) to $(1.4 \pm 0.2) \times 10^7$ CFU/mL was treated by lysozyme and detected by proposed method, the concentration of *Staph. Aureus* is confirmed by plate counting. The response curves of proposed method were shown in Fig. 5a. With the increase of bacteria concentration, the frequency change (ΔF) increased. It can be seen in Fig. 5b that ΔF showed a linear positive relationship with the logarithm of *Staph. Aureus* concentration in range of $(1.4 \pm 0.2) \times 10^2$ to $(1.4 \pm 0.2) \times 10^7$ CFU/mL. Using C represents the concentration of *Staph. Aureus,* the correlation equation was $\Delta F = 14.371 \log_{10} C + 18.212$, a correlation coefficient $R = 0.9563$. The standard deviation of three parallel experiments was in the range of 3.18%–8.9%. The limit of detection (LOD) is 50 CFU/mL, which was determined by the equation $LOD = 3 \times (SD/k)$ (where SD is the standard deviation of the

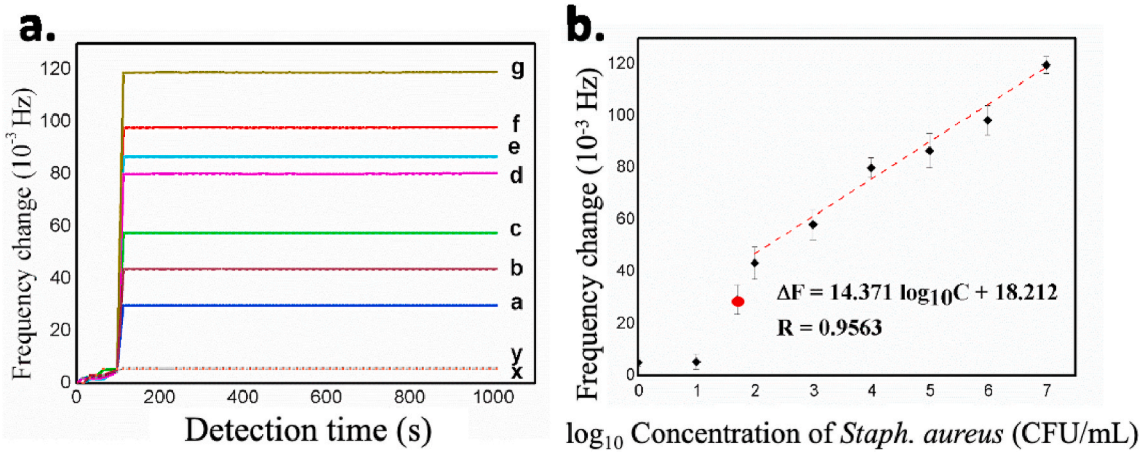

Fig. 5. a. Response curves of different concentration of target bacteria (x, 1.4 CFU/mL; y, $(1.4 \pm 0.2) \times 10$ CFU/mL; a, (50 ± 0.5) CFU/mL; b, $(1.4 \pm 0.2) \times 10^2$ CFU/mL; c, $(1.4 \pm 0.2) \times 10^3$ CFU/mL; d, $(1.4 \pm 0.2) \times 10^4$ CFU/mL; e, $(1.4 \pm 0.2) \times 10^5$ CFU/mL; f, $(1.4 \pm 0.2) \times 10^6$ CFU/mL; g, $(1.4 \pm 0.2) \times 10^7$ CFU/mL); b. Calibration curve for the frequency change of target bacteria in different concentration (logarithmic scale). Error bars indicate standard deviation (n = 3). Red dot: ΔF of 50 CFU/mL *Staph. Aureus.* (For interpretation of the references to color in this figure legend, the reader is referred to the Web version of this article.)

measurement signal for the blank sample, and k is the slope of the analytical curve in the linear region). *Staph. Aureus* at a concentration of 50 ± 0.5 CFU/mL was also detected, the response curve and corresponding ΔF are shown in Fig. 5a and b (red dot), separately. The proposed assay can be accomplished within 100 min, which is far more efficient than the plate counting method (needs more than 24 h).

3.4.2. Specificity study of proposed biosensor

The specificity for bacteria of constructed method was studied by detecting interfering bacteria including *Salmonella enteritidis*, *Escheria coli, Listeria innocua*, *Pseudomonas aeruginosa* and *Streptococcus pneumoniae,* concentration all at $(1.1 \pm 0.5) \times 10^5$ CFU/mL, and mixture bacteria containing five interfering bacteria and *Staph. Aureus,* concentration at $(1.1 \pm 0.5) \times 10^5$ CFU/mL. The detection results were shown in Fig. 6. The degree of interference (DI) of five interfering bacteria to *Staph. Aureus* can be evaluated by formula (1), where ΔF_I and ΔF_T were represented the frequency change of six samples and target bacteria (*Staph. Aureus*). The DI values for *Salmonella enteritidis* (*Sal. Enteritidis*), *Escherichia coli* (*E. coli*), *Listeria innocua (L. innocua*), *Pseudomonas aeruginosa* (*P. aeruginosa*), *Streptococcus pneumoniae* (*S. pneumoniae*) and mixture bacteria sample were 3.24%, 1.55%, 3.43%, 1.70%, 5.04%, and 97.16% respectively, indicating the interference of five bacteria to detection of *Staph. Aureus* could be negligible. There was no significant difference among *Staph. Aureus* results and mixed results. The above results revealed that proposed method is of high specificity for bacteria.

3.5. Detection of target bacteria in simulated human serum and milk sample

A simulated human serum samples and milk samples containing *Staph. Aureus* with a concentration of 50–10^7 CFU/mL were detected using the constructed method, the results were shown in Table 2. The detectable rate of proposed method was varied from 89.00% to 111.33%, which indicated that the proposed method could be used for the detection of bacteria in human serum and milk. The detection limit of *Staph. Aureus* in human serum and milk samples was 50 CFU/mL and the detection time was 100 min.

3.6. Comparison of proposed sensor with representative bacteria detection strategy

A comparison of the performance characteristics for the constructed biosensor and current methods for bacteria detection is presented in Table 3. The results demonstrated the proposed electrochemical sensing strategy possessed simple-operation, fast-response, and high signal-to-noise ratio. Compared with culture method, the proposed bacterial detection method can be accomplished within 100 min, which is far more efficient than the plate counting method (needs more than 24 h). Compared with other molecular biological techniques, the biosensor can detect bacteria in sample which only treated by lysozyme, and all used materials and equipment are facile, all used probes are easy-to-obtain, hence the as-developed method exhibited wide-universality and high-applicability.

In the comparison of typical detection method based on HCR and

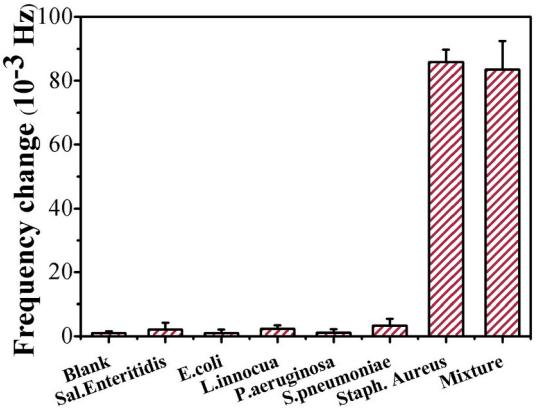

Fig. 6. The effect of interfering bacteria to target bacteria.

Table 2
Detectable rate study of target bacteria measured in simulated samples.

Samples	Added (CFU/mL)	Measured (CFU/mL)	Detectable rate (%)	RSD (%, *n* = 3)
Human serum 1	50	48.53	97.06	5.67
Human serum 2	10^2	$10^{1.78}$	89.00	6.03
Human serum 3	10^3	$10^{3.13}$	104.33	4.38
Human serum 4	10^5	$10^{5.02}$	100.40	2.34
Human serum 5	10^7	$10^{6.58}$	94.00	2.68
Milk 1	50	47.98	95.96	4.38
Milk 2	10^2	$10^{1.83}$	91.50	5.87
Milk 3	10^3	$10^{3.34}$	111.33	2.38
Milk 4	10^5	$10^{4.57}$	91.40	2.71
Milk 5	10^7	$10^{7.13}$	101.86	1.87

Table 3
Comparison of representative bacteria detection strategy.

Method	Detection time	Advantages	Challenges	Ref
culture method	8–48 h	Instrument-free	Tedious, false-negative caused by VBNC microbes	Wang et al. (2015)
polymerase chain reaction	3 h	Super-sensitivity	Limited accuracy	Petralia and Conoci (2017)
gene sequencing	4–24 h	New species classification, high accuracy	Expensive instrument required, complicated operation	Amiri et al. (2018)
immunoassay	100 min	High-specificity, fast-response	Unavailability of monoclonal antibodies	Garvey et al. (2014)
colorimetric method	80 min	Naked-eye detection, free-instrument	Limited sensitivity	Sun et al. (2015)
SERS	20 min	Super-sensitivity, fast-response	Expensive instrument required	Gao et al. (2017)
fluorescent sensor	100 min	High-sensitivity, in-situ detection	Environmental problem of dyes, high cost of dyes	Yang et al. (2018)
MALDI-MS	5 min	Simple operation, fast-response	Expensive instrument required	Blanc et al. (2018)
typical method based on HCR	51 h	High-specificity, simple operation	Relatively high background noise, environmental problem of labels/dyes	Wu et al. (2019)
proposed method based on HCR	100 min	Easy-availability of materials, fast-response, low background noise, easy operation	Lack of naked-eye detection	Presented

proposed method, the typical method based on HCR used HCR as signal amplification technique for nucleic acids analysis by combining signal molecules with repeating units of HCR products, thus the methods are suffered from background noise problem and limited detection reproducibility in complex media such as food or whole blood; while this newly constructed sensor used HCR as tool to connect separated electrodes, thus it exhibits low background noise.

4. Conclusion

In this paper, a novel method with high accuracy and high signal-to-noise ratio is proposed for rapid detection of bacteria by introducing HCR and silver staining techniques into electrochemical signal detection. Utilizing *Staph. aureus* as the representative target bacteria, and MSPQC as the representative electrochemical detector, the proposed method achieves a detection of *Staph. Aureus* over a range from 50 to 10^7 CFU/mL in 100 min with detection limit of 50 CFU/mL. The sample is simply treated by lysozyme, does not need complicated pretreatment including sample dissolution, isolation and purification of nucleic acids. Detection of other bacteria can be done by simply changing the probe corresponding to biomarker. The comparison of constructed biosensor with the current method for bacteria detection were shown in Table 3. The proposed biosensor with its simple operation, fast response, high sensitivity and low background noise offers a great potential for practical applications in public safety monitoring and clinical diagnostics.

CRediT authorship contribution statement

Ye Feng: Conceptualization, Methodology, Formal analysis, Investigation, Writing - original draft. **Dan Zhou:** Software, Methodology, Investigation, Validation. **Lujia Gao:** Data curation, Formal analysis. **Fengjiao He:** Resources, Writing - review & editing, Visualization, Supervision, Project administration, Funding acquisition.

Declaration of competing interest

The authors declare that they have no known competing financial interests or personal relationships that could have appeared to influence the work reported in this paper.

Acknowledgment

This research work was supported by National Natural Science Foundation of China (No. 21275042); Hunan Provincial Science and Technology Department (No. 2015JC3072).

Appendix A. Supplementary data

Supplementary data to this article can be found online at https://doi.org/10.1016/j.bios.2020.112527.

For Table of Contents only

References

Adkins, J.A., Boehle, K., Friend, C., Chamberlain, B., Bisha, B., Henry, C.S., 2017. Colorimetric and electrochemical bacteria detection using printed paper- and transparency-based analytic devices. Anal. Chem. 89, 3613–3621. https://doi.org/10.1021/acs.analchem.6b05009.

Aman, R., Mahas, A., Mahfouz, M., 2020. Nucleic acid detection using CRISPR/cas biosensing technologies. ACS Synth. Biol. https://doi.org/10.1021/acssynbio.9b00507.

Amiri, M., Bezaatpour, A., Jafari, H., Boukherroub, R., Szunerits, S., 2018. Electrochemical methodologies for the detection of pathogens. ACS Sens. 3, 1069–1086. https://doi.org/10.1021/acssensors.8b00239.

Augspurger, E.E., Rana, M., Yigit, M.V., 2018. Chemical and biological sensing using hybridization chain reaction. ACS Sens. 3, 878–902. https://doi.org/10.1021/acssensors.8b00208.

Bai, X., Wu, Z., Josserand, J., Jensen, H., Schafer, H., Girault, H.H., 2004. Passive conductivity detection for capillary electrophoresis. Anal. Chem. 76, 3126–3131. https://doi.org/10.1021/ac035462k.

Bauza, V., Madadi, V., Ocharo, R.M., Nguyen, T.H., Guest, J.S., 2019. Microbial source tracking using 16S rRNA amplicon sequencing identifies evidence of widespread contamination from young children's feces in an urban slum of Nairobi, Kenya. Environ. Sci. Technol. 53, 8271–8281. https://doi.org/10.1021/acs.est.8b06583.

Blanc, L., Lenaerts, A., Dartois, V., Prideaux, B., 2018. Visualization of mycobacterial biomarkers and tuberculosis drugs in infected tissue by MALDI-MS imaging. Anal. Chem. 90, 6275–6282. https://doi.org/10.1021/acs.analchem.8b00985.

Davenport, M., Mach, K.E., Shortliffe, L.M.D., Banaei, N., Wang, T.-H., Liao, J.C., 2017. New and developing diagnostic technologies for urinary tract infections. Nat. Rev. Urol. 14, 296.

Deshmukh, D., Joseph, J., Chakrabarti, M., Sharma, S., Jayasudha, R., Sama, K.C., Sontam, B., Tyagi, M., Narayanan, R., Shivaji, S., 2019. New insights into culture negative endophthalmitis by unbiased next generation sequencing. Sci. Rep. 9, 1–10. https://doi.org/10.1038/s41598-018-37502-w.

Feng, Y., Zhang, X., Su, L., Zhang, Y., He, F., 2019. A supersensitive MSPQC bacterium sensor based on 16S rRNA and "DNA-RNA switch. Biosens. Bioelectron. 138, 111302. https://doi.org/10.1016/j.bios.2019.05.007.

Figg, C.A., Winegar, P.H., Hayes, O.G., Mirkin, C.A., 2020. Controlling the DNA hybridization chain reaction. J. Am. Chem. Soc. 142, 8596–8601. https://doi.org/10.1021/jacs.0c02892.

Furst, A.L., Francis, M.B., 2019. Impedance-based detection of bacteria. Chem. Rev. 119, 700–726. https://doi.org/10.1021/acs.chemrev.8b00381.

Gao, W., Li, B., Yao, R., Li, Z., Wang, X., Dong, X., Qu, H., Li, Q., Li, N., Chi, H., Zhou, B., Xia, Z., 2017. Intuitive label-free SERS detection of bacteria using aptamer-based in situ silver nanoparticles synthesis. Anal. Chem. 89, 9836–9842. https://doi.org/10.1021/acs.analchem.7b01813.

Garvey, G., Shakarisaz, D., Ruiz-Ruiz, F., Hagström, A.E.V., Raja, B., Pascente, C., Kar, A., Kourentzi, K., Rito-Palomares, M., Ruchhoeft, P., Willson, R.C., 2014. Microretroreflector-sedimentation immunoassays for pathogen detection. Anal. Chem. 86, 9029–9035. https://doi.org/10.1021/ac501491t.

He, S., Hong, X., Zhang, M., Wu, L., Yan, X., 2020. Label-free detection of bacteria in fruit juice by nano-flow cytometry. Anal. Chem. 92, 2393–2400. https://doi.org/10.1021/acs.analchem.9b01869.

Hwang, B.H., Shin, H.H., Seo, J.H., Cha, H.J., 2012. Specific multiplex analysis of pathogens using a direct 16S rRNA hybridization in microarray system. Anal. Chem. 84, 4873–4879. https://doi.org/10.1021/ac300476k.

Imai, M., Mine, K., Tomonari, H., Uchiyama, J., Matuzaki, S., Niko, Y., Hadano, S., Watanabe, S., 2019. Dark-field microscopic detection of bacteria using bacteriophage-immobilized SiO2@AuNP core–shell nanoparticles. Anal. Chem. 91, 12352–12357. https://doi.org/10.1021/acs.analchem.9b02715.

Jenkins, J.A., Wax, T.J., Zhao, J., 2017. Seed-mediated synthesis of gold nanoparticles of controlled sizes to demonstrate the impact of size on optical properties. J. Chem. Educ. 94, 1090–1093. https://doi.org/10.1021/acs.jchemed.6b00941.

Kim, S.U., Jo, E.-J., Noh, Y., Mun, H., Ahn, Y.-D., Kim, M.-G., 2018. Adenosine triphosphate bioluminescence-based bacteria detection using targeted photothermal lysis by gold nanorods. Anal. Chem. 90, 10171–10178. https://doi.org/10.1021/acs.analchem.8b00254.

Martynenko, I.V., Kusić, D., Weigert, F., Stafford, S., Donnelly, F.C., Evstigneev, R., Gromova, Y., Baranov, A.V., Rühle, B., Kunte, H.-J., Gun'ko, Y.K., Resch-Genger, U., 2019. Magneto-fluorescent microbeads for bacteria detection constructed from superparamagnetic Fe3O4 nanoparticles and AIS/ZnS quantum dots. Anal. Chem. 91, 12661–12669. https://doi.org/10.1021/acs.analchem.9b01812.

Milioni, D., Mateos-Gil, P., Papadakis, G., Tsortos, A., Sarlidou, O., Gizeli, E., 2020. An acoustic methodology for selecting highly dissipative probes for ultra-sensitive DNA detection. Anal. Chem. https://doi.org/10.1021/acs.analchem.0c00366.

Peng, H., Chen, I.A., 2019. Rapid colorimetric detection of bacterial species through the capture of gold nanoparticles by chimeric phages. ACS Nano 13, 1244–1252. https://doi.org/10.1021/acsnano.8b06395.

Petralia, S., Conoci, S., 2017. PCR technologies for point of care testing: progress and perspectives. ACS Sens. 2, 876–891. https://doi.org/10.1021/acssensors.7b00299.

Ranjbar, S., Nejad, M.A.F., Parolo, C., Shahrokhian, S., Merkoçi, A., 2019. Smart chip for visual detection of bacteria using the electrochromic properties of polyaniline. Anal. Chem. 91, 14960–14966. https://doi.org/10.1021/acs.analchem.9b03407.

Ratajczak, K., Krazinski, B.E., Kowalczyk, A.E., Dworakowska, B., Jakiela, S., Stobiecka, M., 2018. Hairpin–hairpin molecular beacon interactions for detection of survivin mRNA in malignant SW480 cells. ACS Appl. Mater. Interfaces 10, 17028–17039. https://doi.org/10.1021/acsami.8b02342.

Ratajczak, K., Lukasiak, A., Grel, H., Dworakowska, B., Jakiela, S., Stobiecka, M., 2019. Monitoring of dynamic ATP level changes by oligomycin-modulated ATP synthase inhibition in SW480 cancer cells using fluorescent "On-Off" switching DNA aptamer. Anal. Bioanal. Chem. 411, 6899–6911. https://doi.org/10.1007/s00216-019-02061-0.

Ratajczak, K., Stobiecka, M., 2020. High-performance modified cellulose paper-based biosensors for medical diagnostics and early cancer screening: a concise review. Carbohydr. Polym. 229, 115463. https://doi.org/10.1016/j.carbpol.2019.115463.

Reta, N., Saint, C.P., Michelmore, A., Prieto-Simon, B., Voelcker, N.H., 2018. Nanostructured electrochemical biosensors for label-free detection of water- and food-borne pathogens. ACS Appl. Mater. Interfaces 10, 6055–6072. https://doi.org/10.1021/acsami.7b13943.

Slomovic, S., Pardee, K., Collins, J.J., 2015. Synthetic biology devices for in vitro and in vivo diagnostics. Proc. Natl. Acad. Sci. U. S. A 112, 14429–14435. https://doi.org/10.1073/pnas.1508521112.

Stobiecka, M., Chalupa, A., 2016. DNA strand replacement mechanism in molecular beacons encoded for the detection of cancer biomarkers. J. Phys. Chem. B 120, 4782–4790. https://doi.org/10.1021/acs.jpcb.6b03475.

Stobiecka, M., Chałupa, A., 2015. Biosensors based on molecular beacons. Chem. Pap. 69, 62–76. https://doi.org/10.1515/chempap-2015-0026.

Stobiecka, M., Molinero, A.A., Chałupa, A., Hepel, M., 2012. Mercury/homocysteine ligation-induced ON/OFF-switching of a T-T mismatch-based oligonucleotide molecular beacon. Anal. Chem. 84, 4970–4978. https://doi.org/10.1021/ac300632u.

Stobiecka, M., Ratajczak, K., Jakiela, S., 2019. Toward early cancer detection: focus on biosensing systems and biosensors for an anti-apoptotic protein survivin and survivin mRNA. Biosens. Bioelectron. 137, 58–71. https://doi.org/10.1016/j.bios.2019.04.060.

Sun, Q., Zhao, G., Dou, W., 2015. Blue silica nanoparticle-based colorimetric immunoassay for detection of Salmonella pullorum. Anal. Methods 7, 8647–8654. https://doi.org/10.1039/C5AY02073E.

Tavallaie, R., McCarroll, J., Le Grand, M., Ariotti, N., Schuhmann, W., Bakker, E., Tilley, R.D., Hibbert, D.B., Kavallaris, M., Gooding, J.J., 2018. Nucleic acid hybridization on an electrically reconfigurable network of gold-coated magnetic nanoparticles enables microRNA detection in blood. Nat. Nanotechnol. 13, 1066–1071. https://doi.org/10.1038/s41565-018-0232-x.

Wang, J.R., Xia, C., Yang, L., Li, Y.F., Li, C.M., Huang, C.Z., 2020. DNA nanofirecrackers assembled through hybridization chain reaction for ultrasensitive SERS immunoassay of prostate specific antigen. Anal. Chem. 92, 4046–4052. https://doi.org/10.1021/acs.analchem.9b05648.

Wang, Q., Wen, Y., Li, Yan, Liang, W., Li, W., Li, Yuan, Wu, J., Zhu, H., Zhao, K., Zhang, J., Jia, N., Deng, W., Liu, G., 2019. Ultrasensitive electrochemical biosensor of bacterial 16S rRNA gene based on polyA DNA probes. Anal. Chem. 91, 9277–9283. https://doi.org/10.1021/acs.analchem.9b02175.

Wang, Z., Chen, Z., Gao, N., Ren, J., Qu, X., 2015. Transmutation of personal glucose meters into portable and highly sensitive microbial pathogen detection platform. Small 11, 4970–4975. https://doi.org/10.1002/smll.201500944.

Wu, Q., Wang, H., Gong, K., Shang, J., Liu, X., Wang, F., 2019. Construction of an autonomous nonlinear hybridization chain reaction for extracellular vesicles-associated MicroRNAs discrimination. Anal. Chem. 91, 10172–10179. https://doi.org/10.1021/acs.analchem.9b02181.

Yang, L., Deng, W., Cheng, C., Tan, Y., Xie, Q., Yao, S., 2018. Fluorescent immunoassay for the detection of pathogenic bacteria at the single-cell level using carbon dots-encapsulated breakable organosilica nanocapsule as labels. ACS Appl. Mater. Interfaces 10, 3441–3448. https://doi.org/10.1021/acsami.7b18714.

Zhang, W., Wang, L., Yang, Y., Gaskin, P., Teng, K.S., 2019. Recent advances on electrochemical sensors for the detection of organic disinfection byproducts in water. ACS Sens. 4, 1138–1150. https://doi.org/10.1021/acssensors.9b00272.